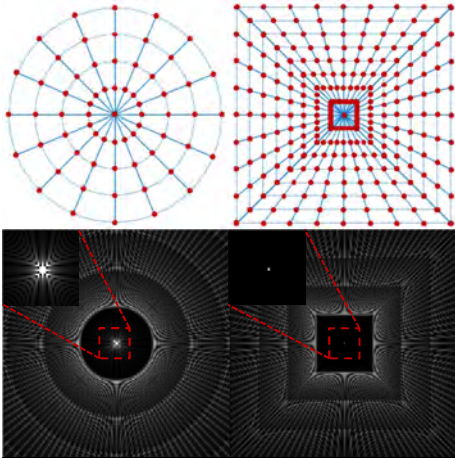


Pseudo-Polar trajectories achieve high acceleration rates with high image fidelity: experiments at 3T and 7T

Ali Ersoz¹ and L Tugan Muftuler^{2,3}

¹Department of Biophysics, Medical College of Wisconsin, Milwaukee, Wisconsin, United States, ²Department of Neurosurgery, Medical College of Wisconsin, Milwaukee, Wisconsin, United States, ³Center for Imaging Research, Medical College of Wisconsin, Milwaukee, Wisconsin, United States

Target Audience: Researchers and users who are interested in non-Cartesian data acquisition and reconstruction



RADIAL, FWHM=1.22 **PPFT**, FWHM=1.00

Fig. 1. PSFs of radial and pseudo-polar sampling

Table 1. Errors in the reconstructed images, $\frac{\|img_{actual} - img_{recon}\|}{\|img_{actual}\|} \times 100$

	RADIAL		PPFT	
	No noise	5% noise	No noise	5% noise
R = 4	6.5%	6.7%	1.3%	3.3%
R = 8	6.7%	7.3%	1.7%	4.6%

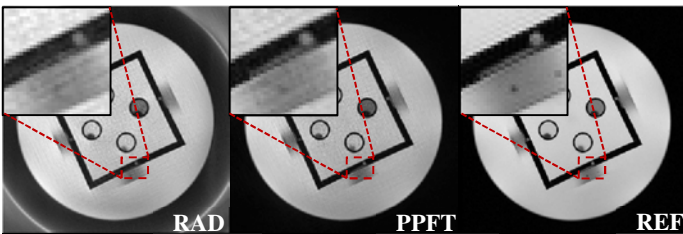


Fig. 2. Experimental phantom images, R=8 (3T, 8-channel coil)

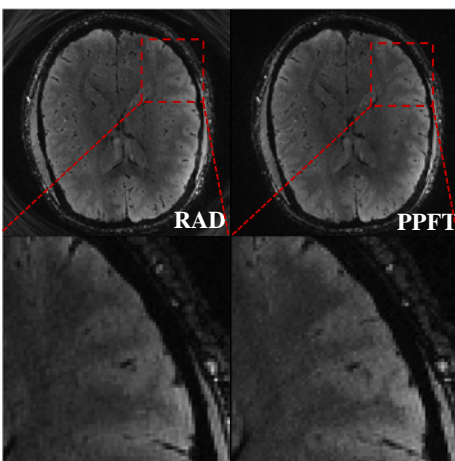


Fig. 3. Brain images, R=4 (7T, 12 virtual coils)

Introduction: Radial imaging has gained more attention recently since it is less prone to subject motion, allows higher acceleration rates with fewer artifacts compared to Cartesian sampling and it covers the center of k-space with each spoke. In radial sampling, the k-space data is first interpolated onto a rectangular grid followed by Fourier Transform. This regridding is necessary since there is no exact transformation between polar grid in k-space and Cartesian grid in image space and errors due to this interpolation step might degrade image quality. However, if data is acquired at equally-sloped spokes (also known as concentric-squares grid) instead of equally-angled, there exists a direct, exact and fast transformation, which is known as Pseudo-Polar Fourier Transform (PPFT)¹. Although these concentric-squares grid methods have been applied to MRI before², a detailed performance comparison to conventional radial sampling has not been done. Especially the undersampling properties and parallel imaging efficacy of these concentric-squares grid methods have not been explored, yet.

Methods: The pseudo-polar grid in k-space is defined by a set of $2n$ spokes, each spoke consisting of $2n$ grid points on n concentric squares for an $n \times n$ image as illustrated in Fig.1. Images from undersampled pseudo-polar data can be reconstructed using any published parallel imaging technique. In this study, we implemented radial GRAPPA for image reconstruction. Kernel sizes and segment sizes for radial and pseudo-polar sampling were selected such that they cover the same area in k-space (2×3 kernel for radial, 2×5 for pseudo-polar). All acceleration rates, R, were given with respect to the Nyquist rate of Cartesian sampling.

Simulations were performed using a Shepp-Logan phantom. First, a no-noise case was implemented and then repeated with noise that had standard deviation equal to 5% of the mean phantom intensity. 256×256 images with R=4 (64 spokes) and R=8 (32 spokes) were reconstructed (for 8-channel RF coil case). The phantom data was acquired in 3T GE Signa Excite MRI system using an 8-channel head coil. Human study (approved by the IRB and written consent was obtained) was performed in 7T GE MR950 scanner using a 32-channel head coil. 32-channel data was compressed into 12 virtual channels before reconstruction. Gradient timing delays were compensated using calibration spokes³. Since PPFT requires $2n$ points on each spoke, bandwidth and FOV were doubled so that gradients and total acquisition time remained the same. Acquisition parameters for phantom and human study were: TE=20ms, TR=200ms, FA=30, FOV=22 and TE=12ms, TR=150ms, FA=15, FOV=20, respectively.

Results and discussion: Point spread function (PSF) plots in Fig.1 shows that pseudo-polar sampling maintains the superior undersampling property of radial sampling. However, in pseudo-polar sampling, artifact-free central region is square-shaped instead of circular. More importantly, the central peak in pseudo-polar sampling is sharper, yielding a FWHM of ~ 1.00 compared to 1.22 in radial sampling. Table 1 lists reconstruction errors of the simulated phantom for both sampling schemes with R=4, 8. The images reconstructed using PPFT has much lower errors compared to radial sampling method. Note that the errors in radial reconstruction remain dominant over the added noise. Fig. 2 illustrates experimental phantom images reconstructed with conventional radial acquisition and PPFT for R=8. A reference image acquired with fully sampled 2D gradient-echo is also shown. The PPFT reconstruction preserved fine details while edges were significantly blurred in conventional radial reconstruction. This is expected since the PSF of PPFT is sharper than the PSF of radial trajectory. Finally, Fig. 3 shows the results from the human study in 7T. It should be noted that the 7T scanner just became available and the acquisition parameters were not optimized for contrast, yet. However, it is still clear that PPFT reconstructed white-matter gray-matter boundaries with higher fidelity. Pseudo-polar trajectories were also shown to have better off-resonance behavior than radial sampling². Therefore, accelerated PPFT could be advantageous in ultra high field MRI systems because of low average SAR, favorable off-resonance behavior and faster acquisition while preserving the image quality at high acceleration rates.

References: [1] A. Averbuch, *et al.* SIAM J. Sci. Comput. 30, 785-803 (2008). [2] N. Gai, *et al.* MRM 37, 275-284(1997) [3] K. T. Block, *et al.* ISMRM 19:2816 (2011)